



## Martian aerosol abundance estimation based on unmixing of hyperspectral imagery

Bin Luo, Xavier Ceamanos, Sylvain Douté, Jocelyn Chanussot

### ► To cite this version:

Bin Luo, Xavier Ceamanos, Sylvain Douté, Jocelyn Chanussot. Martian aerosol abundance estimation based on unmixing of hyperspectral imagery. WHISPERS 2010 - 2nd Workshop on Hyperspectral Image and Signal Processing: Evolution in Remote Sensing, Jun 2010, Reykjavic, Iceland. conference proceedings. hal-00578910

HAL Id: hal-00578910

<https://hal.science/hal-00578910>

Submitted on 22 Mar 2011

**HAL** is a multi-disciplinary open access archive for the deposit and dissemination of scientific research documents, whether they are published or not. The documents may come from teaching and research institutions in France or abroad, or from public or private research centers.

L'archive ouverte pluridisciplinaire **HAL**, est destinée au dépôt et à la diffusion de documents scientifiques de niveau recherche, publiés ou non, émanant des établissements d'enseignement et de recherche français ou étrangers, des laboratoires publics ou privés.

# MARTIAN AEROSOL ABUNDANCE ESTIMATION BASED ON UNMIXING OF HYPERSPECTRAL IMAGERY

Bin Luo<sup>1</sup>, Xavier Ceamanos<sup>2</sup>, Sylvain Douté<sup>2</sup> and Jocelyn Chanussot<sup>1</sup>

<sup>1</sup> Department of Image and Signal, GIPSA-Lab, Grenoble, France

<sup>2</sup> Laboratoire de Planétologie de Grenoble, Grenoble, France

## ABSTRACT

Classical linear unmixing approaches are not valid if the atmosphere and the aerosol are present in hyperspectral data, since the mixture model is no longer linear. In this paper, we present an iterative approach for estimating the abundance of aerosol based on unmixing of Martian hyperspectral data. On one hand, the results can provide the information on the aerosol of the Mars, which is very difficult to obtain. On the other hand, we can use the result to remove the effect of the aerosol on the original image and obtain more accurate linear unmixing results on the surface reflectance.

## 1. INTRODUCTION

Visible and near infrared imaging spectroscopy is a key remote sensing technique to study the Earth and other planets. As solar light is partially transmitted, reflected and diffused back by interaction with the different constituents of the atmosphere and the surface, the analysis of reflectance spectra may allow the identification, quantification, and characterization of the chemical species. In [1], the authors proposed a linear unmixing scheme for unmixing the spectra of the pixels of Martian hyperspectral images in order to identify and quantify the chemical species on the surface of the Mars. However, the mixture of the spectra of the pixels are supposed to be linear. This linear mixture model is valid for the simple surface reflectance. For the intimate mixture of the surface reflectance, the model is no longer linear. More complicated approaches are needed. In [2], it is proposed to use the kernel models in order to quantify the chemical species which are intimately mixed. In addition, the surface reflectance is transmitted by the atmosphere and the aerosol. The transmission is also non linear. In this paper, the spectra received by the sensor are assumed to be the simple surface reflectance (which is usually a linear mixture) transmitted by the atmosphere and the aerosol. The transmission of the gases on the Martian atmosphere is known, since the effect of the atmosphere mainly depends on the topography of the planet. However, the transmission of the aerosol depends on the thickness of the aerosol, which varies according to the captured scene. The objective of this paper is to estimate the abundance of the aerosol as the

optical depth by using linear unmixing approach. The scheme of this paper is presented in Figure 1. Given a hyperspectral image, where the spectra are the surface reflectance transmitted by the atmosphere and the aerosol. We at first correct the transmission effect of the atmosphere and the aerosol by assuming that the thickness of the aerosol is constant in the image. Afterwards, we use the linear unmixing approach to separate the surface reflectance. We then use the results of the linear unmixing for estimating the thickness of the aerosol on each pixel of the image. The above steps make up the first iteration of the algorithm. We then repeat the iteration to improve the accuracy of the estimation of the thickness of the aerosol.

The outline of the paper is as follows: in Section 2, we introduce the mixture model of the received spectra which takes into account the transmission of the atmosphere and the aerosol. In Section 3, the algorithm for estimating the abundance of the aerosol on each pixel is presented. In Section 4, the results of the estimation on synthetic data are presented. Conclusions are presented in Section 5.

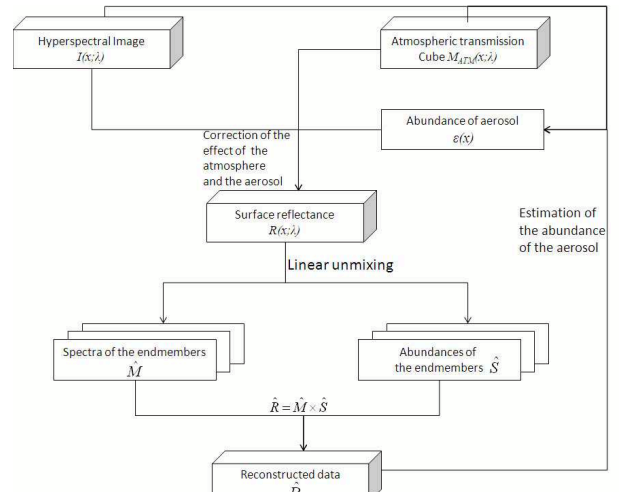


**Fig. 1.** Scheme of the algorithm for estimating of the abundance of the aerosol.

This work is funded by french ANR project VAHINEES.

## 2. NONLINEAR MIXTURE MODEL OF THE ATMOSPHERE AND THE AEROSOL TRANSMISSION ON THE MARS

If we take into consideration the atmosphere and the aerosol transmission, the received reflectance on a pixel  $x$  without noise is:

$$I(x; \lambda) = m_{ATM}(x; \lambda)^{\epsilon(x)} R(x; \lambda), \quad (1)$$

where  $\lambda$  is the wavelength.  $R(x; \lambda)$  is the surface reflectance, which is supposed to be a linear mixture of  $N_c$  endmembers, i.e.

$$R(x; \lambda) = \sum_{i=1}^{N_c} m(x; i) s(i; \lambda) \quad (2)$$

where  $m(x; i)$  is the abundance of the  $i$ th endmember at pixel  $x$  and  $s(i; \cdot)$  is its spectrum.  $m_{ATM}(x; \cdot)$  is the transmission of the atmosphere at pixel  $x$  which mainly depends on the topography of this pixel.  $\epsilon(x)$  is the parameter related to the effect of the aerosol and gas at pixel  $x$  to be estimated, which will be detailed in Section 2.1.

### 2.1. Parameter $\epsilon(x)$

$\epsilon$  can be further decomposed into two terms :

$$\begin{aligned} \epsilon(\theta_0, \theta, \phi, \tau_{aer}, H_{scale}) &= \psi(airmass). \\ &\beta(\theta_0, \theta, \phi, \tau_{aer}, H_{scale}) \end{aligned} \quad (3)$$

where  $\theta_0$ ,  $\theta$  and  $\phi$  are the solar incidence angle, the space-craft emergence angle and the azimuth angle, respectively. In our case, the geometry can only be explained by  $\theta_0$  since OMEGA (carried by Mars Express, 256 spectral bands, 300m resolution) mostly works at nadir. As a consequence,  $\theta$  and  $\phi$  are negligible.  $\tau_{aero}^{k_0}$  is the column integrated opacity of the aerosols and  $H_{scale}$  is the scale height of the distribution. In the experiment,  $H_{scale}$  was set equal to 11.5 km, which is a typical value of Martian polar regions.

The *airmass* represents the distance that the photons travel until reaching the spacecraft and is given by

$$airmass = \frac{1}{\cos(\theta_o)} + \frac{1}{\cos(\theta)} \quad (4)$$

Since we know perfectly  $\phi(airmass)$ , the estimation results of  $\epsilon$  allow us to deduce the effect of the aerosol  $\beta(\theta_0, \theta, \phi, \tau_{aer}, H_{scale})$ , which corresponds directly to the abundance of the aerosol.

## 3. ALGORITHM FOR THE ESTIMATION OF $\epsilon(X)$

We use an iterative scheme for estimating the parameter  $\epsilon(x)$ .

In a first step, the effect of the atmosphere and the aerosol is corrected by assuming that  $\epsilon(x)$  is a constant everywhere

in order to obtain the surface reflectance. In a second step, the linear unmixing approach is used to separate the surface reflectance. In a third step, the results of the linear unmixing are used for estimating the abundance of the aerosol. The result of the estimation is again used to correct the effect of the atmosphere and the aerosol for the next iteration. After a given number of iterations, the algorithm stops. The scheme of the algorithm is shown in Figure 1.

More concretely, we suppose that  $\epsilon_j(x)$  is the  $\epsilon(x)$  estimated after the  $j$ th iteration. We use this value to correct the received spectra in order to obtain the surface reflectance  $R_j(x; \lambda)$  according to Equation (1):

$$R_j(x; \lambda) = \frac{I(x; \lambda)}{m_{ATM}(x; \lambda)^{\epsilon_j}}. \quad (5)$$

Since we suppose that the surface reflectance is a linear mixture of the spectra of several endmembers (see Equation (2)), we can separate the surface reflectance  $R_j$  by using the linear unmixing method – the *Minimum Volume Simplex Analysis* (MVSA) [3]. The sum of the abundances of all the endmembers for each pixel is equal to one, i.e.  $\forall k, \sum_{n=1}^{N_c} s_{n,k} = 1$ , the data vectors  $R_j$  are always inside a simplex of which the vertex are the spectra of the endmembers if there is no noise. The *Vertex Component Analysis* (VCA) which extracts the *extrema* of the simplex as the end-members is proposed in [4] as an efficient algorithm for extracting the endmembers. However, the VCA requires at least one pure pixel (which contains only one endmember) for each endmember. MVSA can find the optimal simplex contains all the data vectors of  $R_j$  and extract its *extrema* as endmembers, even though there is no pure pixel.

By using MVSA, we can obtain the spectra of endmembers  $\hat{m}_j(\cdot; i)$ , as well as their spatial abundances  $\hat{s}_j(i; \cdot)$ . We then reconstruct the surface reflectance by using Equation (2)

$$\hat{R}_j(x; \lambda) = \sum_{i=1}^{N_c} \hat{m}_j(x; i) \hat{s}_j(i; \lambda). \quad (6)$$

Finally we use this reconstruction to re-estimate the parameter  $\epsilon_{j+1}(x)$ . We suppose the optimal  $\epsilon_{j+1}(x)$  minimise the reconstruction error between  $I$  and  $m_{ATM}(x; \lambda)^{\epsilon_{j+1}(x)} R_j(x; \lambda)$ , i.e.

$$\epsilon_{j+1}(x) = \arg \min_{\epsilon \in R} \|I(x; \lambda) - m_{ATM}(x; \lambda)^{\epsilon} R_j(x; \lambda)\|^2. \quad (7)$$

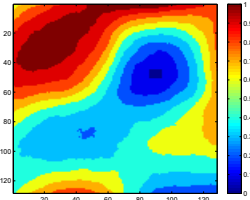
Equation (7) leads to

$$\epsilon_{j+1}(x) = \frac{\sum_{\lambda} m_{ATM}(x; \lambda)(I(x; \lambda) - \hat{R}_j(x; \lambda))}{\sum_{\lambda} m_{ATM}^2(x; \lambda)} \quad (8)$$

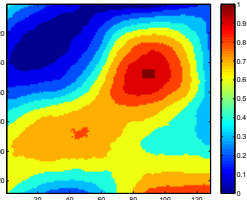
Afterwards, we recompute the updated surface reflectance  $R_{j+1}(x; \lambda)$  for the next iteration by using  $\epsilon_{j+1}(x)$  estimated by Equation (8).

The complete scheme for estimating  $\epsilon(x)$  is then:

- For  $j = 0$  to  $N$



(a) Dust



(b) Water

**Fig. 2.** Ground truth of the abundance of the two endmembers for the simulated image.

- Compute  $R_j$  by using Equation (5);
- Use linear unmixing approach to unmix  $R_j$  for obtaining  $\hat{m}_j$  and  $\hat{s}_j$ ;
- Reconstruct  $\hat{R}_j$  by using Equation (6);
- Update  $\epsilon_{j+1}(x)$  by using Equation (8).
- end

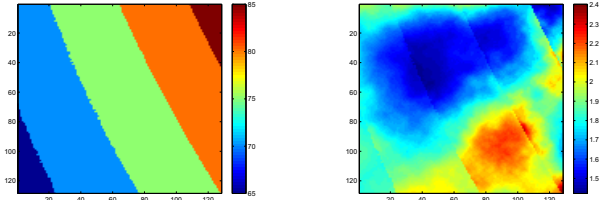
## 4. EXPERIMENTS AND RESULTS

### 4.1. Simulated data

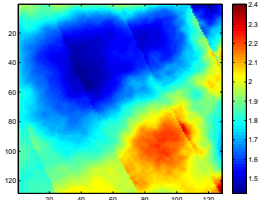
Experiments are performed on a  $128 \times 128$ -pixel synthetic data for evaluation of the aerosol retrieval strategy. Two Martian-like endmembers are present on the surface: water ice and dust. Two complementary abundance maps were generated to simulate a sub-pixel geographic mixture (see Figure 2). Uncertainty was introduced in the data by randomly selecting the grain size of both surface components. Two physical-meaningful ranges of grain size values were chosen according to Martian properties. Then, each surface spectrum was altered by a layer of aerosol which  $\tau_{aero}$  is given by an aerosol abundance map (see Figure 3c). This map was generated by plasma fractals to give a cloud-like realistic result.  $\tau_{aero}$  values were selected from 0.1 to 1.6 to correspond with a Mars-like scenario. Synthetic spectra were differently generated by the method in [5] depending on the value of  $\theta_0$  - from 65 to 85 expressed by the geometry map in Figure 3(a). The high values of *airmass* mimics the polar regions of the Mars. Finally, the surface cube was multiplied by a data set containing the atmospheric transmission of a polar OMEGA image. That was done to reproduce the atmospheric gas effects as well as the topography of the scene. As a matter of fact, the atmospheric contribution on the surface changes depending on the elevation.

### 4.2. Estimation results

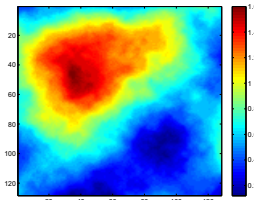
We have performed 3000 iterations (of which the scheme is shown in Section 3) to estimate the  $\epsilon(x)$ . The initial value of  $\epsilon_0 = 2$ , which is between the maximal and the minimal value of the ground truth. In order to evaluate the estimation results, we have computed between the ground truth and each  $\epsilon_j(x)$



(a)

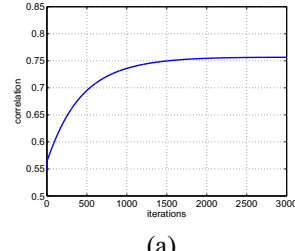


(b)

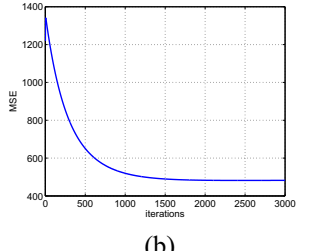


(c)

**Fig. 3.** (a) Incident angle; (b) The ground truth of  $\epsilon(x)$ ; (c) the ground truth of aerosol abundance.



(a)



(b)

**Fig. 4.** (a) Correlation coefficients  $C_j$  between  $\epsilon(x)$  and the estimation results  $\epsilon_j(x)$ ; (b) Mean Square Root Error  $E_j$  between  $\epsilon(x)$  and the estimation results  $\epsilon_j(x)$ ;

obtained at the  $j$ th iteration, the correlation coefficient  $C_j$ , the mean squared error (MSE)  $E_j$  respectively by

$$C_j = \frac{E(\epsilon_j - E(\epsilon_j))(\epsilon - E(\epsilon))}{\sqrt{E(\epsilon_j - E(\epsilon_j))^2 E(\epsilon - E(\epsilon))^2}},$$

$$E_j = E((\epsilon_j - \epsilon)^2).$$

The larger  $C_j$  is, the better  $\epsilon_j(x)$  is, while the smaller  $E_j$  is, the better  $\epsilon_j(x)$  is. In Figure 4, we have shown  $C_j$  and  $E_j$  as the function of iteration step  $j$ . It can be seen that, the correlation coefficient between the estimated  $\epsilon(x)$  and the ground truth always increases (from 0.71 to 0.75), which indicates that the estimated  $\epsilon(x)$  is more and more similar to the ground truth. However, after 1000 iterations, the correlation coefficient increases very slightly. In addition the MSE between the estimated  $\epsilon(x)$  and the ground truth always decreases.

It can be seen that the correlation coefficients always increase. In Figure 5(b), we have shown the  $\epsilon_{3000}(x)$  estimated at the 3000th iteration. For comparison, we have shown in Figure 5(b), the ground truth of the  $\epsilon(x)$  is shown.

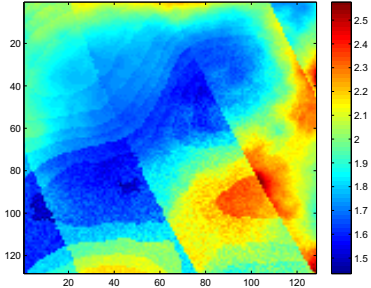


**Fig. 5.** (a) The estimated  $\epsilon_{3000}(x)$  after 3000 iterations

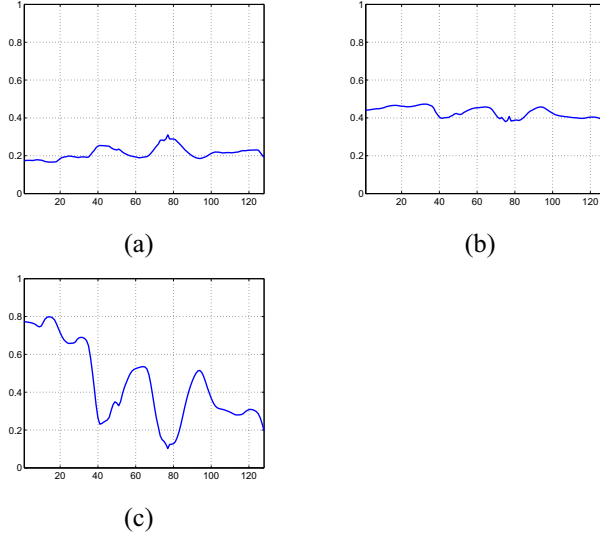
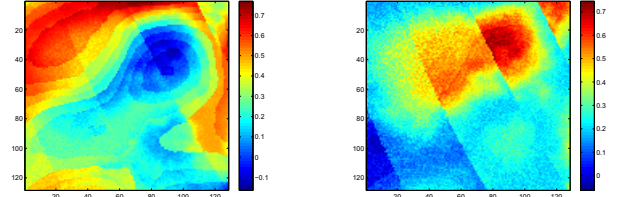


**Fig. 6.** (a)-(c) Spectra of the three endmembers extracted by MVSA after removal of atmosphere and aerosol effect by using  $\epsilon_{3000}(x)$ .

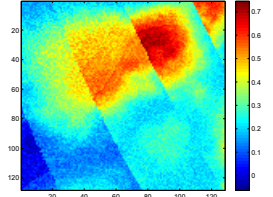
Afterwards, we used MVSA to unmix the surface reflectance  $R_{3000}$  (computed by using Equation (5)). The number of endmember is  $p = 3$ . In Figure 6, we have shown the spectra of these endmembers. It can be seen that the second and the third endmembers correspond to the spectra of the water under different aerosol. While the first endmember is the spectrum of dust. It can be seen that the effect of aerosol decreases a lot for the spectra of water. However, the effect of aerosol is still visible on the extracted spectrum of dust.

Figure 2 shows the ground truth of the two endmembers used for simulating the image.

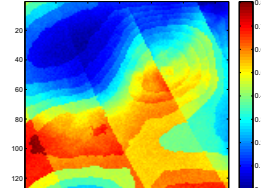
It can be seen that the first abundance map extracted by the linear unmixing (see Figure 7(a)) is approximately the abundance map of the Dust. The other abundance maps extracted by unmixing (see Figure 7(b) and (c)) correspond to the abundance map of the Water.



(a)



(b)



(c)

**Fig. 7.** (a)-(c) Abundances of the three endmembers extracted by MVSA after removal of atmosphere and aerosol effect by using  $\epsilon_{3000}(x)$ .

## 5. CONCLUSION

In this paper, we present an iterative approach for estimating the abundance of aerosol based on unmixing of Martian hyperspectral data. This method is completely statistic without exploiting any information *a priori* on the properties of the surface components. The results obtained from synthetic data show that this approach can provide satisfactory estimation of the abundance of the aerosol. On one hand, the results can provide the information on the aerosol of the Mars, which is very difficult to obtain. On the other hand, we can use the result to remove the effect of the aerosol on the original image and obtain more accurate linear unmixing results on the surface reflectance.

## 6. REFERENCES

- [1] B. Luo, J. Chanussot, and S. Douté, “Unsupervised endmember extraction: Application to hyperspectral images from mars,” in *IEEE ICIP*, Cairo Egypt, 2009.
- [2] J. Broadwater and A. Banerjee, “A comparison of kernel functions for intimate mixture models,” in *WHISPERS09*, Grenoble France, 2009.
- [3] J. Li and J. M. Bioucas-Dias, “Minimum volume simplex analysis: A fast algorithm to unmix hyperspectral data,” in *IGARSS 2008*, Boston USA, 2008, vol. 3, pp. 250–253.
- [4] J. Nascimento and J. M. Bioucas-Dias, “Vertex component analysis: A fast algorithm to unmix hyperspectral data,” *IEEE Trans.on Geoscience and Remote Sensing*, vol. 43, no. 4, pp. 898–910, April 2005.
- [5] S. Douté and B. Schmitt, “A multilayer bidirectional reflectance model for the analysis of planetary surface hyperspectral images at visible and near-infrared wavelengths,” *Journal of Geophysical Research*, vol. 103, no. E13, pp. 31367–31390, 1998.